

# Shape- and Size-Dependent Refractive Index Sensitivity of Gold Nanoparticles

Huanjun Chen, Xiaoshan Kou, Zhi Yang, Weihai Ni, and Jianfang Wang\*

Department of Physics, The Chinese University of Hong Kong, Shatin, Hong Kong SAR, P. R. China

Received January 29, 2008. Revised Manuscript Received April 5, 2008

Gold nanoparticles of different shapes and sizes, including nanospheres, nanocubes, nanobranched, nanorods, and nanobipyramids, were dispersed into water–glycerol mixtures of varying volume ratios to investigate the response of their surface plasmon peaks to the refractive index of the surrounding medium. The refractive index sensitivities and figures of merit were found to be dependent on both the shape and the size of the Au nanoparticles. The index sensitivities generally increase as Au nanoparticles become elongated and their apexes become sharper. Au nanospheres exhibit the smallest refractive index sensitivity of 44 nm/RIU and Au nanobranched exhibit the largest index sensitivity of 703 nm/RIU. Au nanobipyramids possess the largest figures of merit, which increase from 1.7 to 4.5 as the aspect ratio is increased from 1.5 to 4.7.

## Introduction

Noble metal nanoparticles exhibit rich localized surface plasmon resonance properties. Their surface plasmon resonance peaks generally red-shift as the refractive index of the surrounding environment is increased. The dependence of their surface plasmon wavelengths on the surrounding refractive index is highly sensitive, which forms the basis of localized surface plasmon resonance spectroscopy.<sup>1–3</sup> In terms of the detection sensitivity of plasmon spectroscopy, noble metal nanoparticles that exhibit high refractive index sensitivities are strongly desired. A number of efforts have been made to characterize the index sensitivities of Ag nanoparticles of various shapes and sizes. For example, lithographically fabricated Ag nanoparticle arrays have been found to exhibit refractive index sensitivities of  $\sim 200$  nm/RIU.<sup>4–6</sup> The red-shift response of their plasmon resonance peaks to self-assembled alkanethiol monolayers has been found to be linear with a slope of 3 nm per carbon atom.<sup>7–9</sup> Such high sensitivities of Ag nanoparticle arrays have allowed for the fabrication of optical biosensors for the detection of proteins,<sup>10,11</sup> antibodies,<sup>12</sup> and the biomarker for Alzheimer's disease.<sup>13,14</sup> Moreover,

plasmon spectroscopy has been extended to single Ag nanospheres,<sup>15–17</sup> nanocubes,<sup>18</sup> and nanoprisms.<sup>19</sup> Their index sensitivities have been measured to range from 160 to 240 nm/RIU. The use of the single-nanoparticle plasmon sensing technique can reduce the absolute detection limit to the zeptomole level, and an ultrahigh refractive index sensitivity of 4.4-nm red-shift per carbon atom of self-assembled alkanethiol monolayers has been achieved.

Gold nanoparticles are generally more chemically stable than Ag nanoparticles when they are dispersed in aqueous solutions. They are biologically compatible. Their surfaces can be functionalized with a variety of chemical and biological molecules.<sup>20</sup> Moreover, the plasmon resonance wavelengths of Au nanoparticles in various shapes and sizes are on average longer than those of Ag nanoparticles. They can readily be tuned to the near-infrared spectral region, where light penetration into biological tissues is deeper.<sup>21</sup> A number of synthetic methods have been developed for the preparation of Au nanoparticles that have different shapes and sizes.<sup>22–25</sup> However, there have been only a few experimental studies on the refractive index sensitivities of Au nanoparticles.<sup>26–32</sup> A systematic study on the index sensitivities of variously shaped Au nanoparticles is highly desired

\* Corresponding author. Tel: +852 3163 3167. Fax: +852 2603 5204. E-mail: jfwang@phy.cuhk.edu.hk.

- (1) Yonzon, C. R.; Stuart, D. A.; Zhang, X. Y.; McFarland, A. D.; Haynes, C. L.; Van Duyne, R. P. *Talanta* **2005**, *67*, 438.
- (2) Willets, K. A.; Van Duyne, R. P. *Annu. Rev. Phys. Chem.* **2007**, *58*, 267.
- (3) Stewart, M. E.; Anderton, C. R.; Thompson, L. B.; Maria, J.; Gray, S. K.; Rogers, J. A.; Nuzzo, R. G. *Chem. Rev.* **2008**, *108*, 494.
- (4) Jensen, T. R.; Duval, M. L.; Kelly, K. L.; Lazarides, A. A.; Schatz, G. C.; Van Duyne, R. P. *J. Phys. Chem. B* **1999**, *103*, 9846.
- (5) Malinsky, M. D.; Kelly, K. L.; Schatz, G. C.; Van Duyne, R. P. *J. Phys. Chem. B* **2001**, *105*, 2343.
- (6) Haes, A. J.; Zou, S. L.; Schatz, G. C.; Van Duyne, R. P. *J. Phys. Chem. B* **2004**, *108*, 109.
- (7) Malinsky, M. D.; Kelly, K. L.; Schatz, G. C.; Van Duyne, R. P. *J. Am. Chem. Soc.* **2001**, *123*, 1471.
- (8) Haes, A. J.; Zou, S. L.; Schatz, G. C.; Van Duyne, R. P. *J. Phys. Chem. B* **2004**, *108*, 6961.
- (9) Whitney, A. V.; Elam, J. W.; Zou, S. L.; Zinovev, A. V.; Stair, P. C.; Schatz, G. C.; Van Duyne, R. P. *J. Phys. Chem. B* **2005**, *109*, 20522.
- (10) Haes, A. J.; Van Duyne, R. P. *J. Am. Chem. Soc.* **2002**, *124*, 10596.
- (11) Yonzon, C. R.; Jeoung, E.; Zou, S. L.; Schatz, G. C.; Mrksich, M.; Van Duyne, R. P. *J. Am. Chem. Soc.* **2004**, *126*, 12669.
- (12) Riboh, J. C.; Haes, A. J.; McFarland, A. D.; Yonzon, C. R.; Van Duyne, R. P. *J. Phys. Chem. B* **2003**, *107*, 1772.
- (13) Haes, A. J.; Hall, W. P.; Chang, L.; Klein, W. L.; Van Duyne, R. P. *Nano Lett.* **2004**, *4*, 1029.
- (14) Haes, A. J.; Chang, L.; Klein, W. L.; Van Duyne, R. P. *J. Am. Chem. Soc.* **2005**, *127*, 2264.

- (15) Mock, J. J.; Smith, D. R.; Schultz, S. *Nano Lett.* **2003**, *3*, 485.
- (16) McFarland, A. D.; Van Duyne, R. P. *Nano Lett.* **2003**, *3*, 1057.
- (17) Prikulis, J.; Svedberg, F.; Käll, M.; Enger, J.; Ramser, K.; Goksör, M.; Hanstorp, D. *Nano Lett.* **2004**, *4*, 115.
- (18) Sherry, L. J.; Chang, S.-H.; Schatz, G. C.; Van Duyne, R. P.; Wiley, B. J.; Xia, Y. N. *Nano Lett.* **2005**, *5*, 2034.
- (19) Sherry, L. J.; Jin, R. C.; Mirkin, C. A.; Schatz, G. C.; Van Duyne, R. P. *Nano Lett.* **2006**, *6*, 2060.
- (20) Katz, E.; Willner, I. *Angew. Chem., Int. Ed.* **2004**, *43*, 6042.
- (21) Weissleder, R. *Nat. Biotechnol.* **2001**, *19*, 316.
- (22) Daniel, M.-C.; Astruc, D. *Chem. Rev.* **2004**, *104*, 293.
- (23) Pérez-Juste, J.; Pastoriza-Santos, I.; Liz-Marzán, L. M.; Mulvaney, P. *Coord. Chem. Rev.* **2005**, *249*, 1870.
- (24) Murphy, C. J.; Sau, T. K.; Gole, A. M.; Orendorff, C. J.; Gao, J. X.; Gou, L. F.; Hunyadi, S. E.; Li, T. *J. Phys. Chem. B* **2005**, *109*, 13857.
- (25) Liz-Marzán, L. M. *Langmuir* **2006**, *22*, 32.
- (26) Underwood, S.; Mulvaney, P. *Langmuir* **1994**, *10*, 3427.
- (27) Chen, C.-D.; Cheng, S.-F.; Chau, L.-K.; Wang, C. R. *C. Biosens. Bioelectron.* **2007**, *22*, 926.
- (28) Yu, C. X.; Irudayaraj, J. *Biophys. J.* **2007**, *93*, 3684.
- (29) Mayer, K. M.; Lee, S.; Liao, H. W.; Rostro, B. C.; Fuentes, A.; Scully, P. T.; Nehl, C. L.; Hafner, J. H. *ACS Nano* **2008**, Online early access.
- (30) Sun, Y. G.; Xia, Y. N. *Anal. Chem.* **2002**, *74*, 5297.
- (31) Sun, Y. G.; Xia, Y. N. *Analyst* **2003**, *128*, 686.
- (32) Pastoriza-Santos, I.; Sánchez-Iglesias, A.; de Abajo, F. J. G.; Liz-Marzán, L. M. *Adv. Funct. Mater.* **2007**, *17*, 1443.

for realizing ultrasensitive plasmonic sensing with Au nanoparticles. Here, we describe a detailed study on the refractive index sensitivities and figures of merit of five types of differently shaped Au nanoparticles, which are nanospheres, nanocubes, nanobranched, nanorods, and nanobipyramids. Nanorods have three different aspect ratios, and nanobipyramids have four different aspect ratios. The determined index sensitivities range from 44 to 703 nm/RIU, with nanospheres exhibiting the smallest index sensitivity and nanobranched possessing the largest index sensitivity. The determined figures of merit range from 0.6 to 4.5, with nanospheres exhibiting the smallest figure of merit and nanobipyramids possessing the largest figures of merit.

## Experimental Section

### Growth of Gold Nanoparticles with Various Shapes and Sizes.

Gold chloride trihydrate ( $\text{HAuCl}_4 \cdot 3\text{H}_2\text{O}$ ), sodium borohydride ( $\text{NaBH}_4$ ), silver nitrate ( $\text{AgNO}_3$ ), tetradecyltrimethylammonium bromide (TTAB), cetyltrimethylammonium bromide (CTAB), ascorbic acid, and sodium citrate dehydrate were purchased from Sigma-Aldrich. Glycerol was purchased from Farco Chemical Supplies (Beijing, China). Deionized water was used in all the preparations.

Gold nanoparticles of five different shapes, including nanospheres, nanocubes, nanobranched, nanorods, and nanobipyramids, were prepared using a seed-mediated method. Au nanospheres were synthesized according to the method of Gole and Murphy.<sup>33</sup> The resulting Au nanospheres are stabilized with CTAB, positively charged, and have an average diameter of  $(15 \pm 1)$  nm. Au nanocubes were grown following a procedure modified from that reported by Sau and Murphy.<sup>34</sup> Specifically, the seeds were prepared by the addition of a freshly prepared, ice-cold aqueous  $\text{NaBH}_4$  solution (0.01 M, 0.3 mL) into an aqueous mixture solution composed of  $\text{HAuCl}_4$  (0.01 M, 0.125 mL) and CTAB (0.1 M, 3.75 mL), followed by rapid inversion mixing for 2 min. The resulting seed solution was kept at room temperature for 1 h before use. The growth solution was prepared by the sequential addition of CTAB (0.1 M, 6.4 mL),  $\text{HAuCl}_4$  (0.01 M, 0.8 mL), and ascorbic acid (0.1 M, 3.8 mL) into water (32 mL). 20  $\mu\text{L}$  of the CTAB-stabilized seed solution diluted 10 times with water was then added into the growth solution. The resulting solution was mixed by gentle inversion for 10 s and then left undisturbed overnight.

Gold nanobranched were grown with citrate-stabilized Au nanoparticles as seeds. For the preparation of citrate-stabilized seeds, aqueous solutions of  $\text{HAuCl}_4$  (0.01 M, 0.125 mL) and citrate (0.01 M, 0.25 mL) were added into water (9.625 mL), and then a freshly prepared, ice-cold aqueous  $\text{NaBH}_4$  solution (0.01 M, 0.15 mL) was added under vigorous stirring. The resulting seed solution was kept at room temperature for at least 2 h before use. The growth solution of Au nanobranched was prepared by the sequential addition of  $\text{HAuCl}_4$  (0.01 M, 1.8 mL),  $\text{AgNO}_3$  (0.01 M, 0.27 mL), and ascorbic acid (0.1 M, 0.3 mL) into an aqueous TTAB solution (0.1 M, 42.75 mL). The citrate-stabilized seed solution (40  $\mu\text{L}$ ) was then added. The entire reaction solution was mixed by gentle inversion for 10 s and then left undisturbed overnight.

Gold nanorods of three different average aspect ratios were prepared. The nanorods with the largest average aspect ratio,  $4.6 \pm 0.8$ , were grown according to a procedure modified from that reported by Sau and Murphy.<sup>35</sup> Specifically, the seed solution was prepared by the addition of  $\text{HAuCl}_4$  (0.01 M, 0.25 mL) into CTAB (0.1 M, 10 mL) in a 15 mL plastic tube with gentle mixing. A freshly prepared, ice-cold  $\text{NaBH}_4$  solution (0.01 M, 0.6 mL) was then injected quickly into the mixture solution, followed by rapid inversion for 2 min. The seed solution was kept at room temperature for 2 h before use. To grow Au nanorods,  $\text{HAuCl}_4$  (0.01 M, 2.0 mL) and  $\text{AgNO}_3$  (0.01 M, 0.4 mL) were mixed with CTAB (0.1 M, 40 mL) in a 50 mL plastic tube. HCl (1.0 M, 0.8 mL) was then added to adjust the pH of the

solution to 1–2, followed by the addition of ascorbic acid (0.1 M, 0.32 mL). Finally, the CTAB-stabilized seed solution (0.096 mL) was injected into the growth solution. The solution was gently mixed for 10 s and left undisturbed overnight. The nanorods with smaller average aspect ratios,  $2.4 \pm 0.3$  and  $3.4 \pm 0.5$ , were obtained from anisotropic shortening, as reported previously by us.<sup>36</sup>

Gold nanobipyramids of four different average aspect ratios were prepared according to the procedure reported previously by us.<sup>37</sup> They are stabilized with cetyltributylammonium bromide (CTBAB).

**Instrumentation.** Extinction spectra were measured using a Hitachi U-3501 UV–visible/NIR spectrophotometer. Transmission electron microscopy (TEM) images were acquired with a FEI CM120 microscope at 120 kV. Nanoparticle sizes were measured on TEM images. About 200 particles were measured per sample. For TEM characterization, 6 mL of as-grown Au nanoparticle solutions were centrifuged at 11 000 rpm ( $12\,000 \times g$ ) for 6 min. The precipitates were redispersed into water (6 mL each), centrifuged again at 11 000 rpm ( $12\,000 \times g$ ) for 6 min, and finally redispersed into water (0.4 mL each). 0.01 mL of each resulting Au nanoparticle solution was drop-cast carefully onto a lacey-Formvar copper grid stabilized with a thin layer of carbon and allowed to dry in air overnight before TEM imaging.

**Refractive Index Sensitivity Measurement.** Water–glycerol mixtures of varying volume ratios were used to change the refractive index of the surrounding medium of Au nanoparticles. The volume percentage of glycerol in the liquid mixture was varied from 0% to 90% at a step of 10%. As-prepared Au nanoparticles of varying shapes and sizes were first centrifuged at 11 000 rpm ( $12\,000 \times g$ ) for 6 min and then redispersed into the water–glycerol mixture. Extinction spectra of the resulting dispersion solutions of Au nanoparticles were measured. The plasmon shift was plotted as a function of the refractive index, and the refractive index sensitivity was determined by linear fitting. The figure of merit was the index sensitivity divided by the full width at half-maximum of the extinction peak taken from aqueous dispersions of Au nanoparticles.

## Results and Discussions

Gold nanoparticles employed in our experiments were all prepared using a seed-mediated method in the presence of cationic quaternary ammonium surfactants as stabilizing agents. Two types of Au nanoparticle seeds were used. One is stabilized with CTAB, and the other is stabilized with citrate. The former is positively charged, and the latter is negatively charged.<sup>38,39</sup> Au nanospheres, nanocubes, and nanorods were grown using the CTAB-stabilized seeds in the presence of CTAB. Smaller aspect ratio Au nanorods were obtained from anisotropic shortening reaction, where the nanorod diameter remained nearly the same while the length was reduced.<sup>36</sup> The growth of Au nanobranched and nanobipyramids employed the citrate-stabilized seeds. TTAB, which has the same headgroup as CTAB but a shorter hydrophobic tail, was used to stabilize nanobranched during growth. CTBAB, which has the same tail length as CTAB but a larger headgroup, was employed to stabilize nanobipyramids during growth.

Figure 1 shows the typical TEM images of Au nanoparticles of different shapes and sizes. Their yields are shape-dependent, ranging from 50% to 95%. Each nanocube has six surfaces and eight slightly rounded corners. Each nanobipyramid contains 2 sharp tips and 10 side surfaces. Nanobranched contain sharp tips of varying lengths. The number of branched tips per nanobranched ranges from 2 to 8. The sizes of about 200 particles per sample were measured from their TEM images, and the averages are

(36) Tsung, C.-K.; Kou, X. S.; Shi, Q. H.; Zhang, J. P.; Yeung, M. H.; Wang, J. F.; Stucky, G. D. *J. Am. Chem. Soc.* **2006**, *128*, 5352.

(37) Kou, X. S.; Ni, W. H.; Tsung, C.-K.; Chan, K.; Lin, H.-Q.; Stucky, G. D.; Wang, J. F. *Small* **2007**, *3*, 2103.

(38) Liu, M. Z.; Guyot-Sionnest, P. *J. Phys. Chem. B* **2005**, *109*, 22192.

(39) Kou, X. S.; Zhang, S. Z.; Tsung, C.-K.; Yeung, M. H.; Shi, Q. H.; Stucky, G. D.; Sun, L. D.; Wang, J. F.; Yan, C. H. *J. Phys. Chem. B* **2006**, *110*, 16377.

(33) Gole, A.; Murphy, C. J. *Chem. Mater.* **2004**, *16*, 3633.

(34) Sau, T. K.; Murphy, C. J. *J. Am. Chem. Soc.* **2004**, *126*, 8648.

(35) Sau, T. K.; Murphy, C. J. *Langmuir* **2004**, *20*, 6414.

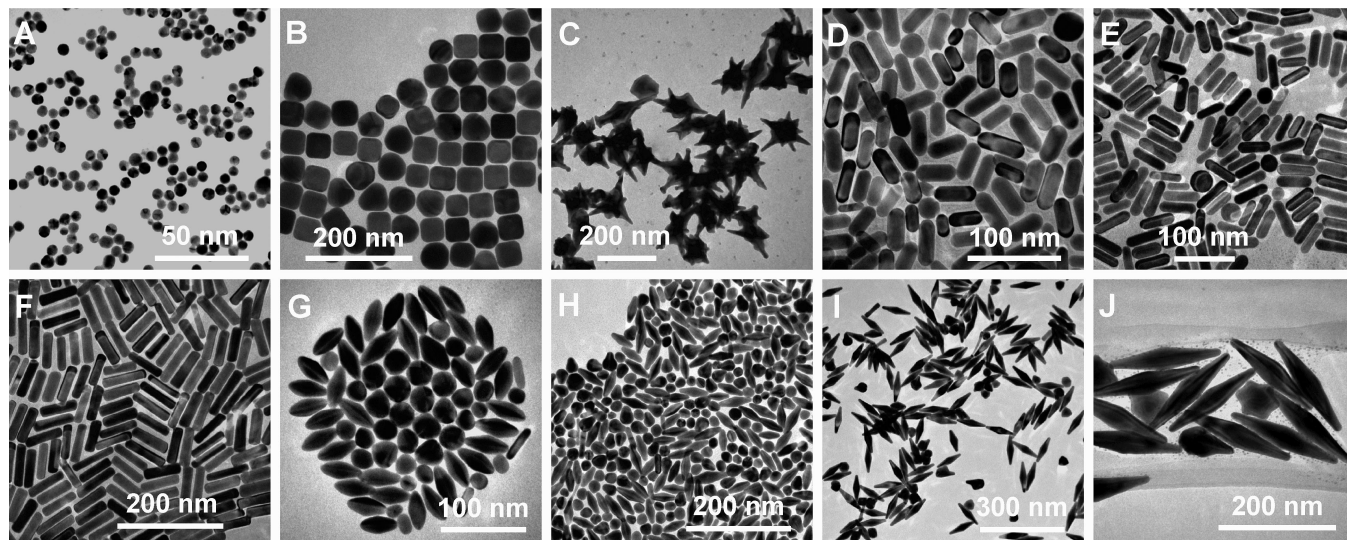


**Figure 1.** Representative TEM images of Au nanoparticles of different shapes and sizes. (A) Nanospheres. (B) Nanocubes. (C) Nanobranches. (D) Nanorods (aspect ratio =  $2.4 \pm 0.3$ ). (E) Nanorods (aspect ratio =  $3.4 \pm 0.5$ ). (F) Nanorods (aspect ratio =  $4.6 \pm 0.8$ ). (G) Nanobipyramids (aspect ratio =  $1.5 \pm 0.3$ ). (H) Nanobipyramids (aspect ratio =  $2.7 \pm 0.2$ ). (I) Nanobipyramids (aspect ratio =  $3.9 \pm 0.2$ ). (J) Nanobipyramids (aspect ratio =  $4.7 \pm 0.2$ ).

**Table 1. Sizes, Plasmon Wavelengths, and Refractive Index Sensitivities of Varily Shaped Au Nanoparticles**

Au nanoparticles	length <sup>a</sup> (nm)	diameter <sup>b</sup> (nm)	aspect ratio <sup>c</sup>	plasmon wavelength <sup>d</sup> (nm)	index sensitivity <sup>e</sup> (nm/RIU)	figure of merit
nanospheres		15 (1)		527	44 (3)	0.6
nanocubes	44 (2)			538	83 (2)	1.5
nanobranches	80 (14)			1141	703 (19)	0.8
nanorods	40 (6)	17 (2)	2.4 (0.3)	653	195 (7)	2.6
nanorods	55 (7)	16 (2)	3.4 (0.5)	728	224 (4)	2.1
nanorods	74 (6)	17 (2)	4.6 (0.8)	846	288 (8)	1.7
nanobipyramids	27 (4)	19 (7)	1.5 (0.3)	645	150 (5)	1.7
nanobipyramids	50 (6)	18 (1)	2.7 (0.2)	735	212 (6)	2.8
nanobipyramids	103 (7)	26 (2)	3.9 (0.2)	886	392 (7)	4.2
nanobipyramids	189 (9)	40 (2)	4.7 (0.2)	1096	540 (6)	4.5

<sup>a</sup> For nanocubes, the edge length was measured. For nanobranches, the length from the center to the branch tip was measured. The numbers in the parentheses are standard deviations. <sup>b</sup> For nanobipyramids, the diameter at the middle was measured. <sup>c</sup> The ratio between the length and the diameter. <sup>d</sup> Measured when Au nanoparticles are dispersed in aqueous solutions. For nanobranches, it is the longer plasmon wavelength. For nanorods and nanobipyramids, it is the longitudinal plasmon wavelength. <sup>e</sup> For nanobranches, it is the refractive index sensitivity of the longer-wavelength plasmon peak. For nanorods and nanobipyramids, it is the index sensitivity of the longitudinal plasmon resonance peak.

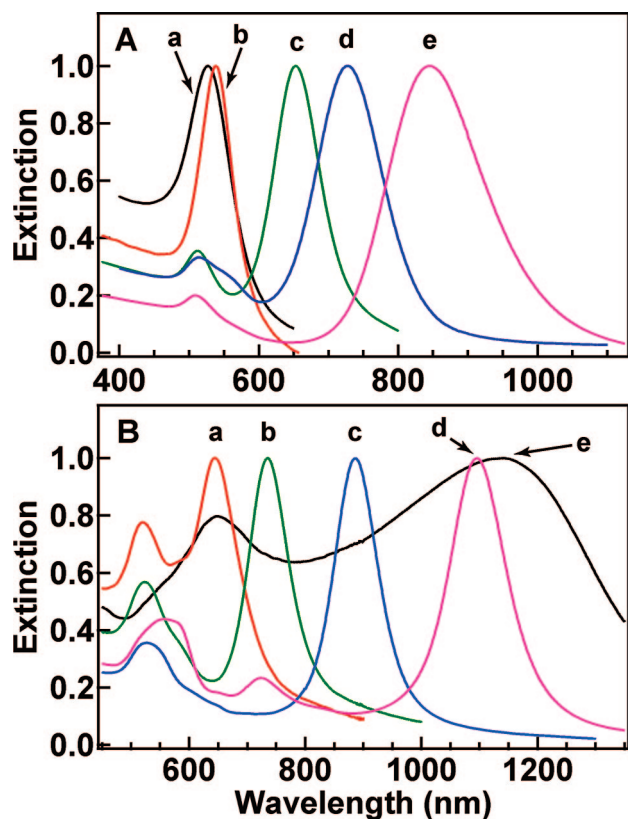
listed in Table 1. These Au nanoparticles cover a wide size range, from 15 to 190 nm, and their size distributions are relatively narrow. For nanocubes, the edge length was measured. For nanobipyramids, the diameter was measured at the middle. For nanobranches, the length from the center to the branched tip was measured and averaged over different branches.

Figure 2 shows the extinction spectra of Au nanoparticles that are stabilized with cationic surfactants in aqueous solutions. Au nanospheres and nanocubes have one surface plasmon peak. Au nanobranches, nanorods, and nanobipyramids exhibit two major surface plasmon peaks. One is associated with electron oscillation along the transverse direction, and the other is associated with electron oscillation along the longitudinal direction. For these elongated nanoparticles, we focus in our experiments on their longitudinal surface plasmon peaks. The surface plasmon peaks of these Au nanoparticles, except nanobranches, are relatively sharp, with their full widths at half-maximum ranging from 50 to 140 nm. Nanobranches have a broad longitudinal plasmon peak, mainly because their tip lengths vary widely within a single nanobranch and among different nanobranches. In addition, a small extinction peak is sometimes observed between the transverse and longitudinal plasmon peaks on the extinction spectra of Au nanobipyramids. This small peak is ascribed to the presence of a small percentage of Au nanorods that are grown

together with Au nanobipyramids.<sup>37</sup> The surface plasmon wavelengths of these nanoparticles are also listed in Table 1. They range from 525 to 1150 nm.

Gold nanoparticles stabilized with cationic quaternary ammonium surfactants are positively charged, because ammonium surfactants form a bilayer on the surfaces of Au nanoparticles, with the ammonium headgroups of one monolayer facing the nanoparticle surfaces.<sup>40</sup> The presence of the surfactant bilayer makes Au nanoparticles very stable when dispersed in aqueous solutions. In order to study the response of their surface plasmon peaks to the refractive index of the surrounding medium, we have tried dispersing Au nanoparticles into organic solvents of varying refractive indexes. When water-immiscible organic solvents, such as chloroform and toluene, are used to disperse Au nanoparticles that are precipitated by centrifugation, they aggregate together, probably because the surfactant bilayer is destroyed in these solvents. When water-miscible solvents, such as methanol and ethanol, are added into aqueous dispersions of Au nanoparticles above a certain volume percentage ( $\sim 30$  vol % for methanol and ethanol), the aggregation of Au nanoparticles occurs immediately. After trying a variety of organic solvents, we have finally found that water-glycerol mixtures can be used

(40) Nikoobakht, B.; El-Sayed, M. A. *Langmuir* **2001**, *17*, 6368.



**Figure 2.** Normalized extinction spectra of Au nanoparticles of different shapes and sizes. (A) Spectra a–e correspond to nanospheres, nanocubes, and nanorods with aspect ratios of  $2.4 \pm 0.3$ ,  $3.4 \pm 0.5$ , and  $4.6 \pm 0.8$ , respectively. (B) Spectra a–e correspond to nanobipyramids with aspect ratios of  $1.5 \pm 0.3$ ,  $2.7 \pm 0.2$ ,  $3.9 \pm 0.2$ , and  $4.7 \pm 0.2$ , and nanobranches, respectively.

to disperse cationic surfactant-stabilized Au nanoparticles without causing aggregation. The volume percentage of glycerol can be up to 100% for the dispersion of Au nanoparticles. In our experiments, the highest volume percentage of glycerol that was used is 90%, because pure glycerol is too viscous.

Figure 3A,B show the extinction spectra of Au nanorods and nanobipyramids dispersed in water–glycerol mixtures of varying volume ratios as two representative examples. As the volume percentage of glycerol is increased, the longitudinal plasmon peaks of Au nanorods and nanobipyramids shift toward the red direction. The longitudinal plasmon wavelengths can be readily obtained from the extinction spectra. The refractive index of the liquid mixture is calculated according to the Lorentz-Lorenz equation:<sup>41</sup>

$$\frac{n_{12}^2 - 1}{n_{12}^2 + 2} = \varphi_1 \frac{n_1^2 - 1}{n_1^2 + 2} + \varphi_2 \frac{n_2^2 - 1}{n_2^2 + 2} \quad (1)$$

where  $n_{12}$  is the refractive index of the liquid mixture,  $n_1$  and  $n_2$  are the indexes of water (1.3334) and glycerol (1.4746), respectively, and  $\varphi_1$  and  $\varphi_2$  are the volume fractions of the two components. The calculated refractive index of the liquid mixture as a function of the volume percentage of glycerol can be fitted well by a line (Supporting Information Figure S1). Figure 3C shows the plots of the plasmon shift, which is the difference between the plasmon wavelengths obtained when Au nanoparticles are dispersed in the liquid mixture and water, respectively, versus the refractive index of the medium for the nanorods and

nanobipyramids shown in Figure 3A,B. Both plots can be fitted well with lines. The slopes of the lines are the refractive index sensitivities. This procedure has been followed to determine the refractive index sensitivities of other Au nanoparticles (Supporting Information Figures S2–S9). The results are summarized in Table 1.

Several observations can be made from the refractive index sensitivities listed in Table 1. (1) The index sensitivities of Au nanospheres and nanocubes are much smaller than those of elongated nanoparticles, such as nanorods, nanobipyramids, and nanobranches. (2) The index sensitivities of both nanorods and nanobipyramids increase with increasing aspect ratios. Since their longitudinal plasmon wavelengths also increase with the aspect ratio,<sup>36,37,42</sup> the use of Au nanorods and nanobipyramids of large aspect ratios for plasmon spectroscopy offers advantages of near-infrared plasmon wavelengths and large index sensitivities. For example, the index sensitivity of the nanorods having a longitudinal plasmon wavelength of 846 nm is 288 nm/RIU and that of the nanobipyramids having a longitudinal plasmon wavelength of 886 nm is 392 nm/RIU. Such index sensitivities are also larger than those determined for single Ag nanoparticles, such as nanospheres,<sup>15,16</sup> nanocubes,<sup>18</sup> and nanoprisms.<sup>19</sup> (3) We have deliberately chosen Au nanorods and nanobipyramids with similar longitudinal plasmon wavelengths (653 versus 645 nm, 728 versus 735 nm, and 846 versus 886 nm) and found that the sensitivities of Au nanobipyramids increase faster than those of the corresponding Au nanorods with increasing longitudinal plasmon wavelengths. This result suggests that the shape and size of Au nanoparticles are also important factors in determining the refractive index sensitivity. (4) The index sensitivities determined for Au nanorods in our experiments are comparable to those measured by Wang et al.<sup>27</sup> (aspect ratio = 5.2, sensitivity = 366 nm/RIU) and Hafner et al.<sup>29</sup> (aspect ratio = 3.3, sensitivity = 170 nm/RIU) and are smaller than those measured by Yu and Irudayaraj<sup>28</sup> (aspect ratio = 2.8–7.0, sensitivity = 450–1150 nm/RIU) at similar aspect ratios. The difference could be because the ends of the Au nanorods used in these experiments are slightly different (see below). (5) In general, the index sensitivity increases as the apexes of Au nanoparticles get sharper. Au nanobranches with the sharpest tips exhibit the highest index sensitivity, up to 703 nm/RIU. More experiments are required to see how the index sensitivity of Au nanobranches varies with the length of the branched tips and the number of tips per nanobranch. New synthetic methods are also needed to prepare Au nanobranches of narrow size distributions for the use in plasmon spectroscopy. The index sensitivities could be further increased by making metal nanostructures of sharper apexes, as have been demonstrated with nanorices<sup>43</sup> (801 nm/RIU) and nanocrescents<sup>44</sup> (up to 880 nm/RIU), and employing plasmon-coupled metal nanostructures.<sup>45</sup> (6) The figures of merit of Au nanobipyramids are much larger than those of Au nanorods, which is because nanobipyramids have larger index sensitivities and more uniform size than nanorods. Au nanobipyramids should therefore be more advantageous than Au nanorods when nanoparticle ensembles are employed for plasmonic sensing.

(42) Kou, X. S.; Zhang, S. Z.; Yang, Z.; Tsung, C.-K.; Stucky, G. D.; Sun, L. D.; Wang, J. F.; Yan, C. H. *J. Am. Chem. Soc.* **2007**, *129*, 6402.

(43) Wang, H.; Brandl, D. W.; Le, F.; Nordlander, P.; Halas, N. J. *Nano Lett.* **2006**, *6*, 827.

(44) Bukasov, R.; Shumaker-Parry, J. S. *Nano Lett.* **2007**, *7*, 1113.

(45) Stewart, M. E.; Mack, N. H.; Malyarchuk, V.; Soares, J. A. N. T.; Lee, T.-W.; Gray, S. K.; Nuzzo, R. G.; Rogers, J. A. *Proc. Natl. Acad. Sci. U.S.A.* **2006**, *103*, 17143.

(41) Mehra, R. *Proc. Indian Acad. Sci. (Chem. Sci.)* **2003**, *115*, 147.

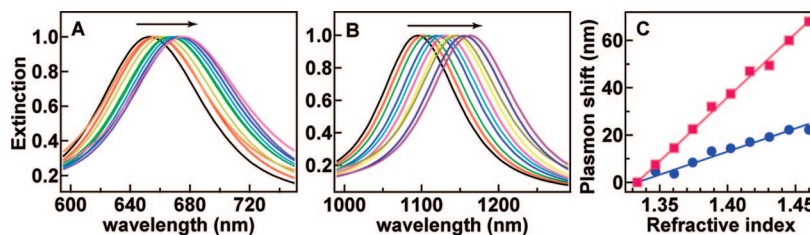


**Figure 3.** (A) Extinction spectra of Au nanorods (aspect ratio =  $2.4 \pm 0.3$ ) in water–glycerol liquid mixtures of varying compositions. (B) Extinction spectra of Au nanobipyramids (aspect ratio =  $4.7 \pm 0.2$ ) in water–glycerol liquid mixtures of varying compositions. Each spectrum is normalized to its maximal extinction intensity. The arrows indicate the direction of increasing volume percentage of glycerol. (C) Dependence of the longitudinal plasmon shift on the refractive index of the liquid mixture for the Au nanorods (blue circles) and nanobipyramids (red squares) shown in (A) and (B), respectively. The lines are linear fits.

### Conclusions

Water–glycerol liquid mixtures of varying volume ratios were found to be able to disperse cationic surfactant-stabilized Au nanoparticles without causing aggregation. Au nanoparticles of different shapes and sizes, including nanospheres, nanocubes, nanobranched, nanorods, and nanobipyramids, were dispersed into water–glycerol mixtures; and the response of their surface plasmon peaks to the refractive index of the surrounding medium was investigated. The refractive index sensitivities and figures of merit were found to be dependent on the shape and size of Au nanoparticles. The index sensitivities range from 44 to 703 nm/RIU and generally increase as the apexes of Au nanoparticles get sharper. Au nanospheres exhibit the smallest index sensitivity, and Au nanobranched exhibit the largest index sensitivity. The figures of merit range from 0.6 to 4.5, with nanospheres exhibiting

the smallest figure of merit and nanobipyramids possessing the largest figures of merit. These results are of implications for the design and fabrication of ultrasensitive plasmonic chemical and biological sensors.

**Acknowledgment.** This work was supported by the RGC Research Grant Direct Allocation (Project Code: 2060306) and a RGC CERG grant (ref. no.: 403006, project code: 2160293).

**Supporting Information Available:** Refractive index change of water–glycerol mixtures, extinction spectra of Au nanoparticles of different shapes and sizes in water–glycerol mixtures of varying compositions, and the dependence of the plasmon shift on the refractive index of the liquid mixture. This material is available free of charge via the Internet at <http://pubs.acs.org>.

LA800305J

# Shape- and Size-Dependent Refractive Index Sensitivity of Gold Nanoparticles

Huanjun Chen, Xiaoshan Kou, Zhi Yang, Weihai Ni, and Jianfang Wang\*

## Supporting Information

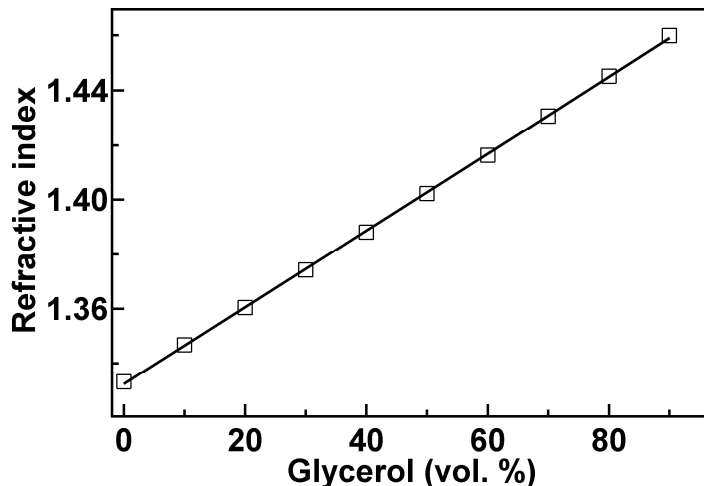


**Figure S1.** Dependence of the refractive index of water-glycerol mixtures on the volume percentage of glycerol. The line is a linear fit.

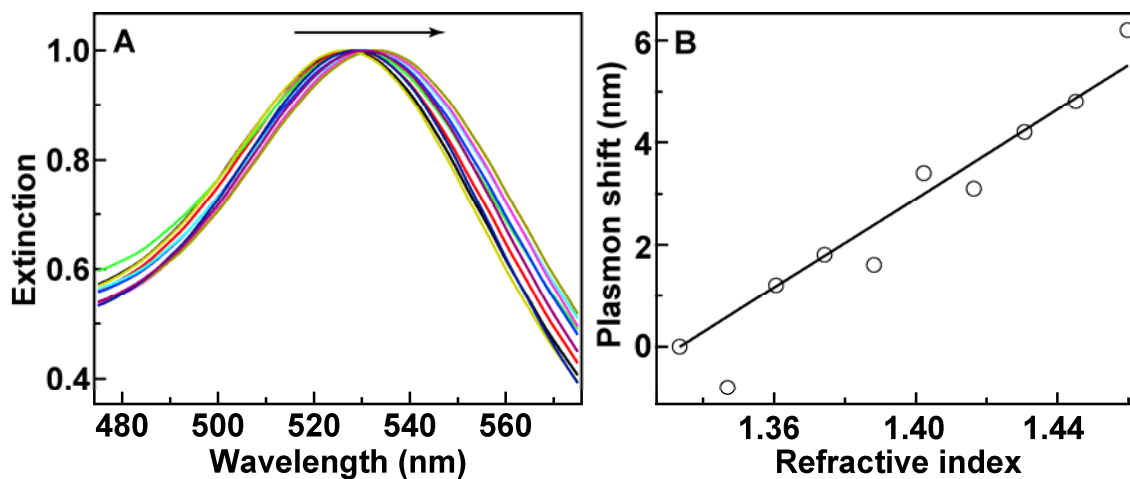


**Figure S2.** (A) Normalized extinction spectra of Au nanospheres dispersed in water-glycerol mixtures of varying compositions. The arrow indicates the direction of increasing volume percentage of glycerol in the liquid mixture. (B) Dependence of the plasmon shift on the refractive index of the liquid mixture. The line is a linear fit.

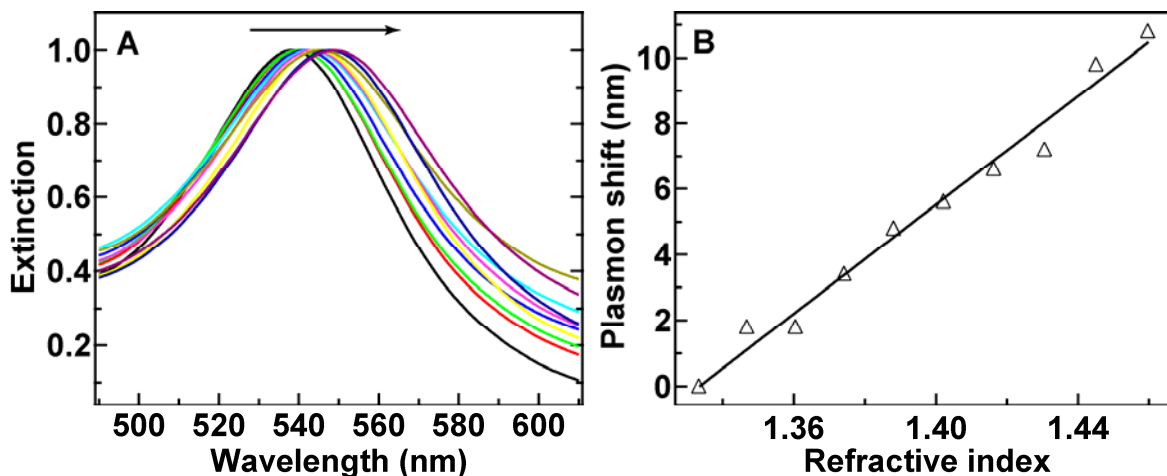


**Figure S3** (A) Normalized extinction spectra of Au nanocubes dispersed in water-glycerol mixtures of varying compositions. The arrow indicates the direction of increasing volume percentage of glycerol in the liquid mixture. (B) Dependence of the plasmon shift on the refractive index of the liquid mixture. The line is a linear fit.

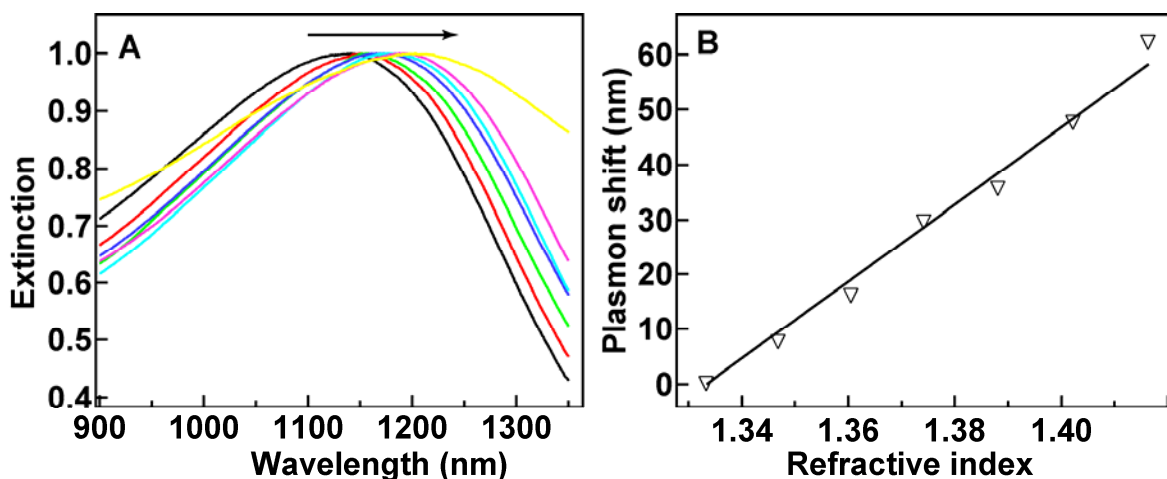


**Figure S4.** (A) Normalized extinction spectra of Au nanobranched structures in water-glycerol mixtures of varying compositions. The arrow indicates the direction of increasing volume percentage of glycerol in the liquid mixture. Au nanobranched structures exhibit aggregation when the volume percentage of glycerol is higher than 60 vol. %. (B) Dependence of the plasmon shift on the refractive index of the liquid mixture. The line is a linear fit.

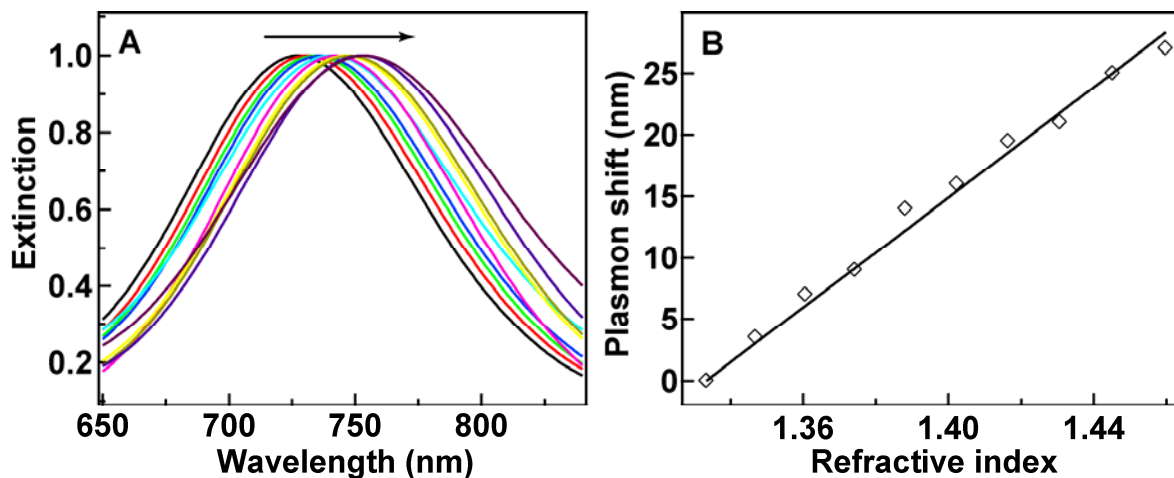


**Figure S5.** (A) Normalized extinction spectra of Au nanorods with an aspect ratio of  $3.4 \pm 0.5$  in water-glycerol mixtures of varying compositions. The arrow indicates the direction of increasing volume percentage of glycerol in the liquid mixture. (B) Dependence of the longitudinal plasmon shift on the refractive index of the liquid mixture. The line is a linear fit.

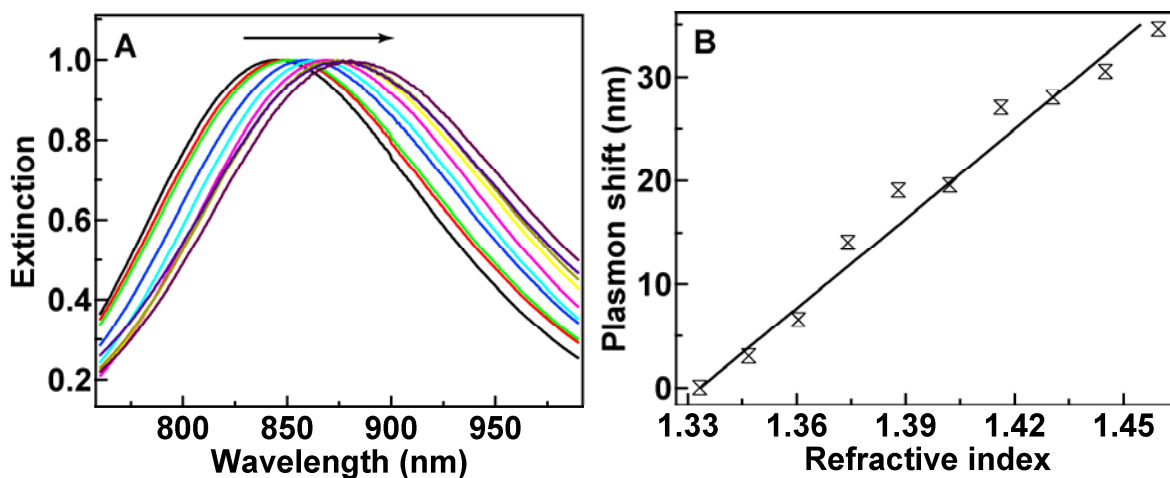


**Figure S6.** (A) Normalized extinction spectra of Au nanorods with an aspect ratio of  $4.6 \pm 0.8$  in water-glycerol mixtures of varying compositions. The arrow indicates the direction of increasing volume percentage of glycerol in the liquid mixture. (B) Dependence of the longitudinal plasmon shift on the refractive index of the liquid mixture. The line is a linear fit.

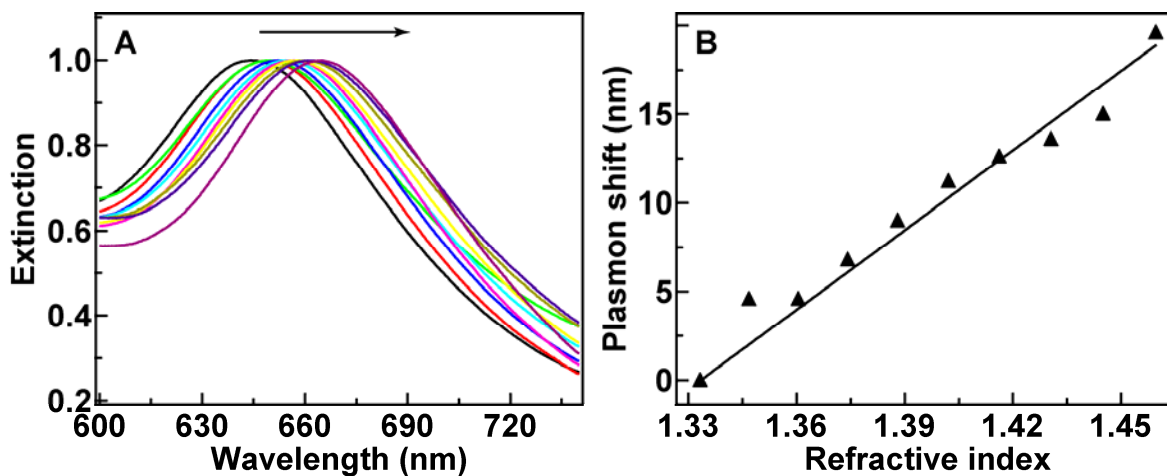


**Figure S7.** (A) Normalized extinction spectra of Au nanobipyramids with an aspect ratio of  $1.5 \pm 0.3$  in water-glycerol mixtures of varying compositions. The arrow indicates the direction of increasing volume percentage of glycerol in the liquid mixture. (B) Dependence of the longitudinal plasmon shift on the refractive index of the liquid mixture. The line is a linear fit.

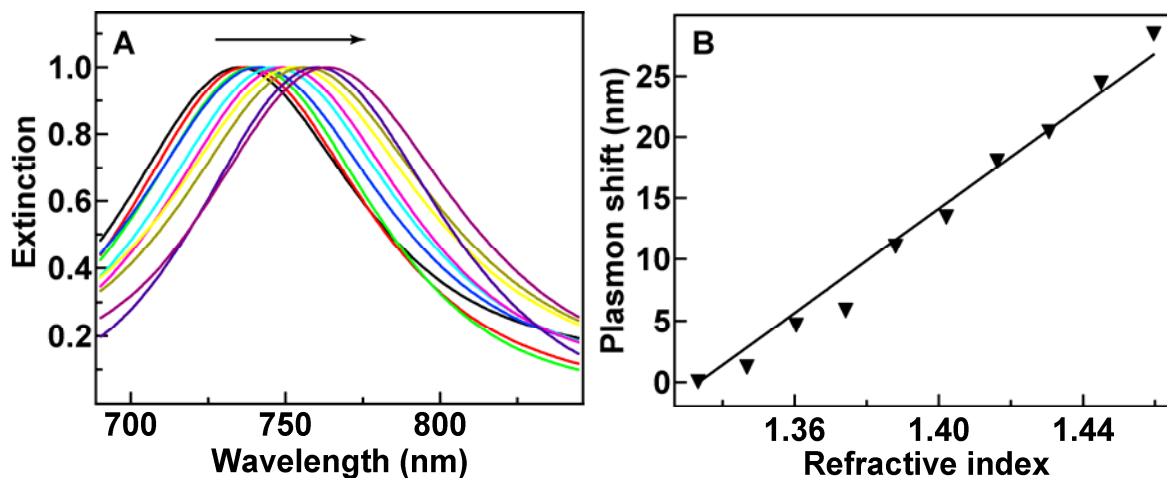


**Figure S8.** (A) Normalized extinction spectra of Au nanobipyramids with an aspect ratio of  $2.7 \pm 0.2$  in water-glycerol mixtures of varying compositions. The arrow indicates the direction of increasing volume percentage of glycerol in the liquid mixture. (B) Dependence of the longitudinal plasmon shift on the refractive index of the liquid mixture. The line is a linear fit.

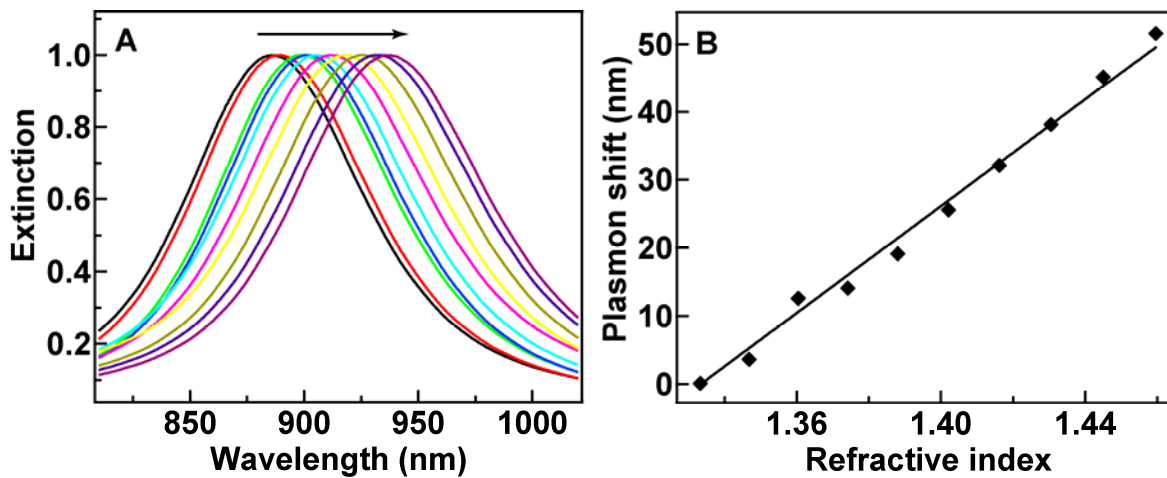


**Figure S9.** (A) Normalized extinction spectra of Au nanobipyramids with an aspect ratio of  $3.9 \pm 0.2$  in water-glycerol mixtures of varying compositions. The arrow indicates the direction of increasing volume percentage of glycerol in the liquid mixture. (B) Dependence of the longitudinal plasmon shift on the refractive index of the liquid mixture. The line is a linear fit.